Sweet-Parker Reconnection with Anomalous Resistivity — A Toy Model

Xue-Ning Bai (Princeton)

August 22, 2010

Faculty advisor: Pattrick Diamond (UCSD)

Abstract

Magnetic reconnection is a common phenomenon in astrophysical contexts. The conventional Sweet-Parker model describes magnetic reconnection due resistivity. However, microscopic resistivity appears too small to reproduce the observed rate of reconnection. In this report, we describe the basic idea of anomalous resistivity in non-relativistic collisionless ion-electron plasma. We build a one-dimensional model along the direction of current in the current sheet. When the ion temperature is much less than the electron temperature, ion-acoustic instability develops when current density is sufficiently large so that the electron drift speed exceeds a few times the sound speed. The instability generates ion-acoustic waves, which are damped by non-linear wave-particle interaction. Anomalous resistivity arises due to the momentum exchange between waves and particles. The calculated anomalous resistivity strongly depends on the current density in the current sheet, and is typically much larger than the microscopic resistivity. However, matching the anomalous resistivity to the Sweet-Parker model, the resulting reconnection rate still falls off the observed rate by a large factor.

1 Sweet-Parker Reconnection: An Overview

Magnetic reconnection describes the process of changing magnetic field topology due to non-ideal MHD effects. A typical example is a pair of oppositely directed field lines break and reattach themselves as they approach each other. It usually involves magnetic dissipation and conversion of magnetic energy to plasma kinetic energy. Be the kinetic energy thermal, it produces plasma heating. In the collisionless regime, the conversion tends to produce a population of non-thermal particles, which is an important mechanism for particle acceleration.

Magnetic reconnection takes place in a large variety of astrophysical environments, including the corona of accretion disks (protostellar disk, AGN disk, and disks around compact objects), MHD turbulence, magnetospheres of stars, planets and compact objects, gamma-ray burst, etc. To study magnetic reconnection, it is important to distinguish between various different regimes. For example, the plasma can be composed of ions and electrons, or electron-positron pairs. The plasma velocity can be non-relativistic or relativistic, and the reconnection can be collisional or collisionless. In this report, we study the magnetic reconnection for the "conventional" non-relativistic ion-electron collisionless plasma.

1.1 Sweet-Parker Model for Magnetic Reconnection

The Sweet-Parker model describes the steady-state magnetic reconnection of oppositely directed magnetic fields due to resistivity (Sweet, 1958; Parker, 1957), as we sketch below. More details can be found in Kulsrud (2005), Zweibel & Yamada (2009) and Yamada et al. (2010).

Let B_0 be the strength of the field far from the current sheet, 2δ be the sheet thickness, and η be the resistivity. Therefore, the current density in the sheet is

$$j \approx \frac{cB_0}{4\pi\delta} \ , \tag{1}$$

and the Ohmic heating rate equals

$$\dot{Q} = Ej = \frac{4\pi\eta j^2}{c^2} = \frac{\eta B_0^2}{4\pi\delta^2} \ . \tag{2}$$

The heating increases the plasma pressure in the current sheet, which balances the loss of magnetic pressure due to the reconnection. Let $2L$ be the length scale of the current sheet. Since L is finite, a pressure gradient along the current sheet pushes the plasma to flow alongside at about the Alfvén speed $v_A = B_0/\sqrt{4\pi\rho}$ (shock will develop if the speed is larger). Since the plasma is heated for $t_h \approx L/v_A$, the pressure gain is

$$\Delta p \approx \dot{Q} t_h = \frac{\eta B_0^2}{4\pi\delta^2} \frac{L}{v_A} \ . \tag{3}$$

Pressure equilibrium requires $\Delta p = B_0^2/8\pi$, from which we obtain

$$\delta \approx \sqrt{\frac{\eta L}{v_A}} = \frac{L}{\sqrt{S}} \ , \tag{4}$$

where we have dropped a factor $\sqrt{2}$ since the estimate is only approximate, and S is the Lundquist number

$$S \equiv \frac{L v_A}{\eta} \ , \tag{5}$$

which is the ratio of magnetic diffusion time scale to the Alfvén time scale. Equation (4) sets a lower limit on the current sheet thickness since in reality one expects $\Delta p < B_0^2/8\pi$.

Due to mass conservation, the mass flux out of the reconnection region $2\delta v_A$ has to be balanced by the mass inflow $2Lv_R$, where v_R is the velocity of the incoming plasma, found to be

$$v_R = \frac{\delta}{L} v_A = \frac{v_A}{\sqrt{S}} = \sqrt{\frac{v_A \eta}{L}} \ . \tag{6}$$

Note that the reconnection rate scales as $\sqrt{\eta}$.

The Sweet-Parker picture of magnetic reconnection is only qualitative. However, it provides important scaling relations between the rate of reconnection and resistivity, and has definite predictions, as we discuss in the next subsection. A more quantitative realization of the Sweet-Parker reconnection is given in Uzdensky & Kulsrud (2000), where it was found that the correction factor for equation (6) is only 1.07.

1.2 Comparison with Observations

The Sweet-Parker model leads to reconnection time scale shorter than the resistive decay time scale by a factor of $\sqrt{S}$, while longer than the Alfvén time scale by a factor of $\sqrt{S}$, and can be made direct comparison with observations. Below we provide two classical examples (Kulsrud, 2005).

1.2.1 Solar Flares

A solar flare is a large explosion in the surface of the Sun, heating the plasma to tens of millions of Kelvin, and produce radiation across the electromagnetic spectrum at all wavelengths as well as charged particles up to very high energies. Most flares occur in active regions around the sunspots. They are powered by the sudden release of magnetic energy stored in the solar corona as a consequence of magnetic reconnection.

We can estimate the reconnection time scale from the Sweet-Parker model using some possible parameters relevant for the solar flare:

$$L \sim 10^5 \mathrm{km} \ , \qquad \rho \sim 10^{-14} \mathrm{g\ cm^{-3}} \ , \qquad B \sim 100 \mathrm{G} \ , \qquad T \sim 10^7 \mathrm{K} \ . \tag{7}$$

From the above we find

$$n \sim 2.5 \times 10^9 \mathrm{cm^{-3}} \ , \qquad v_A \sim 3 \times 10^8 \mathrm{cm\ s^{-1}} \ , \qquad \tau_e \sim 10 \mathrm{s} \ . \tag{8}$$

where the electron collision time is estimated from Braginskii (1965). The Ohmic resistivity can be obtained by

$$\eta_O = \frac{c^2 m_e}{4\pi n e^2 \tau_e} \sim 10 \mathrm{cm^2 s} \ . \tag{9}$$

The Lundquist number is therefore $S \sim 10^{17}$, and we have

$$\delta_{\rm SP} \sim 30 \mathrm{cm} \ , \qquad \tau_{\rm SP} = \sqrt{S} \frac{L}{v_A} \sim 10^{10} \mathrm{s} \ . \tag{10}$$

However, the observed time scale of the solar flare is of the order 10^4s, which is 6 orders of magnitude smaller than the Sweet-Parker model predictions.

1.2.2 Earth Magnetosphere

In the Earth magnetosphere, the magnetic field advected by the solar wind reconnects with Earth's magnetic field in the day side. The reconnected field lines are then gradually advected to the night side of the Earth, and reconnect again (Hughes, 1995). As the Earth rotates, the reconnection process reaches a steady state such that the loss of magnetic flux in the day side is balanced by the re-supply in the night side.

Similarly, we can find the parameters relevant for the reconnection in the Earth's magnetosphere:

$$L \sim 10^3 \mathrm{km} \ , \qquad \rho \sim 10^{-21} \mathrm{g\ cm^{-3}} \ , \qquad B \sim 10^{-4} \mathrm{G} \ , \qquad T \sim 10^7 \mathrm{K} \ . \tag{11}$$

From the above we find

$$n \sim 3 \times 10^2 \mathrm{cm^{-3}} \ , \qquad v_A \sim 10^6 \mathrm{cm\ s^{-1}} \ , \qquad \tau_e \sim 5 \times 10^4 \mathrm{s} \ , \qquad \eta_O \sim 2 \times 10^4 \mathrm{cm^2 s} \ . \tag{12}$$

Further, we have $S \sim 5 \times 10^9$ and

$$\delta_{\rm SP} \sim 10^3 \mathrm{cm} \ , \qquad \tau_{\rm SP} =\sim 7 \times 10^6 \mathrm{s} \ , \qquad v_R = \frac{v_A}{\sqrt{S}} \sim 20 \mathrm{cm\ s^{-1}} \ . \tag{13}$$

The speed of the solar wind is about $v_w \sim 200 \mathrm{km\ s^{-1}}$, which implies that about $v_R/v_w \sim 10^{-6}$ of the field lines reconnect. However, the fraction of reconnected field lines as inferred from counting the number of field lines crossing the poles is about $5 - 10$ percent, which is 5 orders of magnitude more than the Sweet-Parker model predictions.

1.3 Making Reconnection Faster

As we have seen from the previous subsection, the Sweet-Parker model with microscopic resistivity predicts the reconnection that is too slow compared with observations. To match the observed rate of reconnection, one has to go beyond the conventional Sweet-Parker model to seek for faster reconnection rate, and we list three ideas below.

1. Petschek's model for fast reconnection (Petschek, 1964). The basic idea is that reconnection may proceed mainly through a narrow channel of thickness δ, rather than L. Consequently, reconnection can proceed at much larger speed, and the outflow velocity from the reconnecting region is super-Alfvénic which gives rise to shocks.

2. Anomalous resistivity. The current in the current sheet implies free energy extractable by current-driven plasma micro-instabilities. Plasma waves are excited by the instabilities and are damped due to non-linear effects, which leads to weak turbulence. Anomalous resistivity arises from the momentum exchange between particles and waves, which is generally much larger than microscopic resistivity. We will focus on and elaborate this idea throughout this report.

3. Hall reconnection. Hall physics becomes important correction to resistive MHD when the current sheet thickness δ is less than the ion skin depth c/ω_{pi}. For ion-electron plasma, the mass flux is carried by the ions, while the magnetic flux is controlled by the electrons. When $\delta < c/\omega_{pi}$, ions can flow in wider channel of width c/ω_{pi}, hence larger rate of reconnection.

Numerical simulations show that Petschek's reconnection occurs only when resistivity is strongly spatially variable (Malyshkin et al., 2005), but does not show up in the case of constant resistivity. Signatures of both anomalous resistivity and Hall effects are observed in laboratory experiments, depending on collisionalities and instruments (see the review by Zweibel & Yamada, 2009). Finally, we note that the above three ideas are not independent with each other. For example, since anomalous resistivity generally depends on current density, it can also lead to Petschek's reconnection. Also, both anomalous resistivity and two-fluid (Hall) effect can be present simultaneously.

The rest of this report is organized as follows. We stick to the idea of anomalous resistivity by building an 1D model along the direction of current. The wave excitation mechanism is due to the ion-acoustic instability, which is formulated and discussed in §2. Wave-particle interaction is discussed in §3, which exchanges energy and momentum between waves and particles and acts as the wave damping mechanism. The anomalous resistivity arisen from the wave-particle interaction is calculated in §4, which is further compared with constraints from observations. We summarize in §5.

2 Plasma Basics for Ion-Acoustic Instability

2.1 Basic Formulation for Linear Waves

We consider collisionless plasma with zero guide field as appropriate for the reconnection current sheet. As an approximation, we assume constant current density $\boldsymbol{j}$, along the $\hat{x}$ direction. Let $f_i(\boldsymbol{x},\boldsymbol{v},t)$ and $f_e(\boldsymbol{x},\boldsymbol{v},t)$ be the distribution function of ions and electrons respectively. We use subscript "$_0$" to denote the background distribution, which is uniform in space and time. They are assumed to be Maxwellian, with ion and electron temperatures denoted by T_i and T_e. We work in the frame where the ion drift velocity is zero. Therefore, the electron drift speed satisfies $j = n_0 e v_d$, where n_0 is the background electron/ion density $n_0 = \int f_0 d^3v$. The background distribution functions read

$$f_{0i}(\boldsymbol{v}) = \frac{n_0}{(2\pi v_i^2)^{3/2}} \exp\left(-v^2/2v_i^2\right) , \qquad f_{0e}(\boldsymbol{v}) = \frac{n_0}{(2\pi v_e^2)^{3/2}} \exp\left\{-[(v_x - v_d)^2 + v_y^2 + v_z^2]/2v_e^2\right\} , \tag{14}$$

where we denote the ion and electron thermal velocities $v_{ti}^2 \equiv kT_i/m_i$ and $v_{te} \equiv kT_e/m_e$. Since we work in 1D, it is useful to integrate the distribution functions over y and z to obtain

$$F_{0i}(v_x) = \frac{n_0}{\sqrt{2\pi}v_i} \exp\left(-v_x^2/2v_i^2\right) , \qquad F_{0e}(v_x) = \frac{n_0}{\sqrt{2\pi}v_e} \exp\left[-(v_x - v_d)^2/2v_e^2\right] , \tag{15}$$

where the capital F denotes the integrated distribution function.

Suppose the system obeys the background distribution for $t < 0$. Perturbations to the distribution function denoted by subscript "$_1$" are introduced at $t = 0$. We consider only **electrostatic** perturbations where there is no perturbation to the magnetic field. Electromagnetic waves propagate near the speed of light and is not likely to be relevant to anomalous resistivity in non-relativistic plasma. To the first order, the perturbation equations read

$$\frac{\partial f_{1e}}{\partial t} + \boldsymbol{v}\cdot\nabla f_{1e} = \frac{e}{m_e}\boldsymbol{E}\cdot\nabla_v f_{0e} , \qquad \frac{\partial f_{1i}}{\partial t} + \boldsymbol{v}\cdot\nabla f_{1i} = -\frac{e}{m_i}\boldsymbol{E}\cdot\nabla_v f_{0i} , \tag{16}$$

$$\nabla \cdot \boldsymbol{E} = 4\pi(n_i - n_e)e = 4\pi e \int (f_{1i} - f_{1e}) d^3v \ , \tag{17}$$

Note that for 1D problem, $\boldsymbol{E}$ has only $\hat{x}$ component.

To proceed, we decompose the perturbed electric field into Fourier modes

$$\overline{E}(k,t) = \frac{1}{2\pi} \int E(x,t) e^{-\mathrm{i}kx} dx \ , \qquad E(x,t) = \int \overline{E}(k,t) e^{\mathrm{i}kx} dk \ , \tag{18}$$

where spatial Fourier components are marked with " $\bar{}$ ". For simplicity, we consider only a single k mode with amplitude $\overline{E}(k,t)$ below, and the perturbation equations now read

$$\frac{\partial \overline{F}_1}{\partial t} + \mathrm{i}kv_x \overline{F}_1 = -\frac{q}{m} \overline{E} \frac{\partial F_0}{\partial v_x} \ , \tag{19}$$

$$\mathrm{i}k\overline{E} = 4\pi e \int (\overline{F}_{1i} - \overline{F}_{1e}) dv_x \ . \tag{20}$$

Note that we have integrated the distribution functions over y and z, and for conciseness, we have omitted subscript "i" and "e" and use $q = \pm e$ to denote ion/electron charge.

Next, we perform **Laplace transformation** on t, and the corresponding components are marked with " $\tilde{}$ ". The transformation on E reads

$$\widetilde{E}(k,\varpi) = \int_0^\infty \overline{E}(k,t) e^{\mathrm{i}\varpi t} dt \ , \qquad \overline{E}(k,t) = \frac{1}{2\pi} \int_{-\infty+\mathrm{i}\mu}^{\infty+\mathrm{i}\mu} \widetilde{E}(k,\varpi) e^{-\mathrm{i}\varpi t} d\varpi \ , \tag{21}$$

where $\varpi \equiv \omega + \mathrm{i}\mu$ with ω and $\mu > 0$ being real. The transformation on equation (19) leads to

$$-\overline{F}_1(v_x,t)\Big|_{t=0} - \mathrm{i}(\varpi - kv_x)\widetilde{F}_1(k,\varpi) = -\frac{q}{m}\widetilde{E}\frac{\partial F_0}{\partial v_x} \ , \tag{22}$$

so that

$$\widetilde{F}_1(k,v_x,\varpi) = \frac{\mathrm{i}\overline{F}_1(v_x,0)}{\varpi - kv_x} - \frac{\mathrm{i}q}{m}\frac{\widetilde{E}(k,\varpi)}{\varpi - kv_x}\frac{\partial F_0}{\partial v_x} \ . \tag{23}$$

Substituting this equation to equation (20), we obtain

$$\epsilon(k,\varpi)\widetilde{E}(k,\varpi) = \frac{4\pi e}{k} \int \frac{\overline{F}_{1i}(v_x,0) - \overline{F}_{1e}(v_x,0)}{\varpi - kv_x} dv_x \equiv J(k,\varpi) \ , \tag{24}$$

where the dielectric constant

$$\epsilon(k,\varpi) = 1 + \frac{4\pi e^2}{m_i k} \int \frac{dv_x}{\varpi - kv_x} \frac{\partial F_{0i}}{\partial v_x} + \frac{4\pi e^2}{m_e k} \int \frac{dv_x}{\varpi - kv_x} \frac{\partial F_{0e}}{\partial v_x} \ . \tag{25}$$

Therefore, we obtain

$$\overline{E}(k,t) = \frac{1}{2\pi} \int_{-\infty+\mathrm{i}\mu}^{\infty+\mathrm{i}\mu} \frac{J(k,\varpi)}{\epsilon(k,\varpi)} e^{-\mathrm{i}\varpi t} d\varpi \ . \tag{26}$$

In order to perform the integration (26), one can analytically continue $\epsilon(k,\varpi)$ and other functions (e.g., $J(k,\varpi)$) to the entire complex plane. Note that the original Laplace transformation requires Im $\varpi > 0$. Analitical continuation means that **in performing the integral on ϖ, one has to enclose the zeros of $\epsilon(k,\varpi)$ from above** (assuming the zeros of ϵ are on or below the real axis, as is almost always the case), while **performing the integral on v_x, the integration path must enclose ϖ/k from below**.

2.2 Plasma Waves

In this subsection, we ignore the electron drift relative to the ions (i.e., set $j = 0$ and $v_d = 0$ for simplicity, although the dispersion relation does not depend on v_d in proper frames) and discuss the plasma waves without worrying about Landau damping (see §2.3). In this case, the Laplace transformation reduces to Fourier transformation (i.e., $\mu = 0$, $\varpi = \omega$). Recall that the definition of

the dielectric constnat comes from $\nabla \times \boldsymbol{B}_1 = -\mathrm{i}(\omega/c)\boldsymbol{\epsilon} \cdot \boldsymbol{E}_1$. Therefore, for electrostatic waves, the dispersion relation is simply obtained by $\epsilon(k,\omega) = 0$.

First consider cold plasma, i.e., $v_i = v_e = 0$. Integrating equation (25) by parts, we easily obtain

$$\epsilon(k,\omega) = 1 - \frac{\omega_{pi}^2}{\omega^2} - \frac{\omega_{pe}^2}{\omega^2} \ , \tag{27}$$

where $\omega_p^2 = 4\pi e^2 n_0/m$ is the plasma frequency. Therefore, the dispersion relation is simply $\omega^2 = \omega_{pe}^2 + \omega_{pi}^2 \approx \omega_{pe}^2$, which is just plasma oscillation, and the frequency is independent of k.

Next, we relax the condition of cold plasma by allowing non-zero temperature but $v_i, v_e \ll |\omega/k|$. In this case, we can expand $(\omega - kv_x)^{-1}$ as

$$\frac{1}{\omega - kv_x} \approx \frac{1}{\omega}\left(1 + \frac{kv_x}{\omega} + \frac{k^2 v_x^2}{\omega^2} + \frac{k^3 v_x^3}{\omega^3}\right) . \tag{28}$$

Substituting the Maxwellian distribution into equation (25), we find the dispersion relation

$$\omega^2 = \omega_{pe}^2 + \frac{3k^2 v_e^2}{\omega^2}\omega_{pe}^2 + \omega_{pi}^2 + \frac{3k^2 v_i^2}{\omega^2}\omega_{pi}^2 \approx \omega_{pe}^2 + 3k^2 v_e^2 \ , \tag{29}$$

The second term on the right is called the **Bohm-Gross correction** due to the thermal effects. The group velocity of the wave is

$$v_g = \frac{\partial \omega}{\partial k} \approx \frac{3kv_e^2}{\omega_{pe}} = 3k\lambda_D v_e \ , \tag{30}$$

where $\lambda_D = v_e/\omega_{pe}$ is the Debye length. Note that the group (phase) velocity is larger (smaller) for small wavelength.

In the above two cases, ions play an insignificant role in the wave properties. Finally, consider the opposite limit $v_i \ll \omega/k \ll v_e$. For electrons, we can approximate $(\omega - kv_x)^{-1}$ as $-1/kv_x$. In such limits, we find the dispersion relation to be

$$1 = \frac{\omega_{pi}^2}{\omega^2} - \frac{\omega_{pe}^2}{k^2 v_e^2} \ , \tag{31}$$

or

$$\frac{\omega^2}{\omega_{pi}^2} = \frac{k^2\lambda_D^2}{1 + k^2\lambda_D^2} \ , \qquad \text{or} \qquad \omega^2 = \frac{k^2 c_s^2}{1 + k^2\lambda_D^2} \ , \tag{32}$$

where $c_s \equiv \sqrt{m_e/m_i}v_e$. This is the **ion-acoustic wave**, which corresponds to the longitudinal oscillation of the ions. In the long wavelength (compared with Debye length) limit, it reduces to sound waves.

Later we will discuss the energy exchange between waves and particles. The wave energy density is proportional to the square of the electric field. Averaging over the volume gives

$$\frac{1}{L}\int_{-L/2}^{L/2} E(x)^2 dx = \frac{1}{L}\int_{-L/2}^{L/2} dx \int dk dk' \widetilde{E}(k)\widetilde{E}(k') e^{\mathrm{i}(k+k')x} = \int dk \widetilde{I}(k) dk \ , \tag{33}$$

where L is the size of the system and $\widetilde{I}(k)$ is the "intensity" of the electric vector per unit wave number

$$\widetilde{I}(k) \equiv \frac{|\widetilde{E}(k)|^2}{L} \ , \tag{34}$$

With this definition, now we quote the action density per unit wave number as

$$N_k = \frac{1}{\omega}\frac{\partial}{\partial \omega}[\omega\epsilon(k,\omega)]\frac{\widetilde{I}(k)}{8\pi} \ . \tag{35}$$

The energy and momentum density of the waves per unit wave number is then

$$\mathscr{E}_w(k) = \omega N_k = \omega \left.\frac{\partial \epsilon}{\partial \omega}\right|_{\epsilon=0} \frac{\widetilde{I}(k)}{8\pi} \ , \tag{36}$$

$$\mathscr{P}_w(k) = k N_k \ , \tag{37}$$

where the second equality in equation (36) applies only to electrostatic waves.

2.3 Landau Damping

Now we work on the general case and discuss the integral (26). One can extend the integration path into a contour, closed from the lower half plane with Im $\varpi \to -\infty$. Note that the extended part of the path integrates to zero, then according to the residue theorem, we have

$$\overline{E}(k,t) = \mathrm{i} \sum_{\epsilon(k,\varpi_n)=0} \frac{J(k,\varpi)}{\partial\epsilon/\partial\varpi} e^{-\mathrm{i}\varpi t}\bigg|_{\varpi=\varpi_n} , \tag{38}$$

where ϖ_ns are all the zeros of the dielectric function $\epsilon(k,\varpi)$ in the complex plane. Note that in general ϵ has multiple roots, thus Fourier transformation with single frequency does not work in this problem, which explains why Laplace transformation is used here.

Let $\varpi_1 = \omega_1 + \mathrm{i}\mu_1$ be the root with the largest imaginary part μ_1. Then the long-term behavior of the electric field is

$$\overline{E}(k,t) \sim e^{-\mathrm{i}\omega_1 t + \mu_1 t} . \tag{39}$$

Therefore, $\mu_1 < 0$ leads to the damping of the wave, as is often the case, which is called **Landau damping**. Conversely, if $\mu_1 > 0$, the modes grow exponentially, which is called **inverse Landau damping**, or Landau growth. The most important point is that **the behavior of the perturbation is completely determined by the zeros of the dielectric function**.

Next we apply this result to the problem of plasma oscillation with resonant particles. To avoid complications, we choose k to be small so that the wave phase velocity is large compared with the electron thermal velocity and the number of resonant particles is small. To the zeroth order (neglecting the effect of resonance), we have the Bohm-Gross root (29), denoted by $\varpi = \omega_0 \approx \omega_{pe}$. To the first order of the resonant interactions, we write $\varpi = \omega_0 + \varpi_1$, and decompose the dielectric constant into the real and imaginary parts $\epsilon = \epsilon_R + \mathrm{i}\epsilon_I$. From the previous subsection, we have

$$\epsilon_R(k,\varpi) \approx 1 - \frac{\omega_{pe}^2 + 3k^2 v_e^2}{\varpi^2} , \qquad \frac{\partial\epsilon_R}{\partial\varpi}\bigg|_{\omega_0} = \frac{2}{\omega_0} . \tag{40}$$

Note that $kv_e \ll \omega_{pe}$ and the contribution from the ions is negligible. The imaginary part ϵ_I at $\varpi = \omega_0$ can be obtained by integrating over a semicircle around ω_0/k from below

$$\mathrm{i}\epsilon_I(k,\omega_0) = -\mathrm{i}\pi \frac{4\pi e^2}{k^2 m_e} \frac{\partial F_{0e}}{\partial v_x}\bigg|_{\omega_0/k} - \mathrm{i}\pi \frac{4\pi e^2}{k^2 m_i} \frac{\partial F_{0i}}{\partial v_x}\bigg|_{\omega_0/k} . \tag{41}$$

Then, the first order correction for the root can be obtained by setting $\epsilon_R(\omega_0 + \varpi_1) + \mathrm{i}\epsilon_I(\omega_0) = 0$, which gives

$$\varpi_1 = -\frac{\mathrm{i}\epsilon_I(\omega_0)}{\partial\epsilon_R/\partial\omega_0} , \tag{42}$$

where we have used $\epsilon_R(\omega_0) = 0$. Therefore, we find for the exponential growth rate

$$\mu_1 = \varpi_1/\mathrm{i} = \frac{2\pi^2 e^2 \omega_0}{k^2} \left[\frac{1}{m_e}\frac{\partial F_{0e}}{\partial v_x} + \frac{1}{m_i}\frac{\partial F_{0i}}{\partial v_x}\right]\bigg|_{\omega_0/k} = \frac{\pi\omega_0}{2n_0 k^2} \left[\omega_{pe}^2 \frac{\partial F_{0e}}{\partial v_x} + \omega_{pi}^2 \frac{\partial F_{0i}}{\partial v_x}\right]\bigg|_{\omega_0/k} . \tag{43}$$

Once again, this result applies only when ω_0/k is far from the peak of the distribution function F_0 for both electrons and ions so that the expansion (28) is applicable.

It is important to note that whether the plasma waves grow or damp depends on the sign of $\omega_0 \partial F_0/\partial v_x$. Physically, particles traveling slightly faster than the wave are slowed down, giving energy to the wave, and conversely, particles traveling slightly slower than the wave are accelerated, extracting energy from the wave. For a right-moving wave ($\omega_0 > 0$) whose phase velocity is in the thermal tail of the Maxwellian distribution ($\partial F_0/\partial v_x < 0$), this always leads to damping. Let us ignore the ion for the moment, and work in the frame of the electrons. Assuming Maxwellian distribution, we have $\partial F_{0e}/\partial v_x = -(v_x/v_e^2)F_{0e}$, thus

$$\frac{\mu_1}{\omega_0} = -\frac{\sqrt{\pi}}{2\sqrt{2}} \frac{\omega_0 \omega_{pe}^2}{k^3 v_e^3} \exp\left(-\frac{\omega_0^2}{2k^2 v_e^2}\right) = -\frac{\sqrt{\pi/8}}{k^3 \lambda_D^3} e^{-1/2k^2\lambda_D^2} . \tag{44}$$

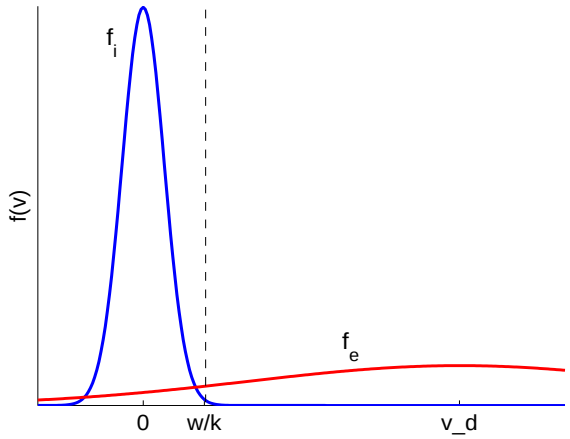

Figure 1: Illustration of the ion-acoustic instability. f_i and f_e denotes the ion and electron distribution function, ω/k labels the wave phase velocity, and v_d is the electron drift speed.

Note that our formula applies in the regime $k\lambda_D \ll 1$, and the damping rate is small due to the exponential factor.

2.4 Ion-Acoustic Instability

In the example of the previous subsection, we considered the damping of plasma oscillations. In this subsection we consider the ion-acoustic waves, and we also take into account the electron drift velocity relative to the ions v_d. Again, we work in the regime $v_i \ll \omega/k$ and $|\omega/k - v_d| \ll v_e$. Similar as before, the zeroth order dielectric constant can be found in equation (31), with ω_0 given in equation (32) (note that the electron drift velocity does not contribute under our approximations). Correspondingly, we have

$$\left.\frac{\partial \epsilon_R}{\partial \varpi}\right|_{\omega_0} = \frac{2\omega_{pi}^2}{\omega_0^3} \,. \tag{45}$$

The imaginary part of the dielectric function is the same as (41), therefore, we obtain the growth rate from equation (42)

$$\frac{\mu}{\omega_0} = \frac{\pi\omega_0^2}{2n_0k^2}\left[\frac{m_i}{m_e}\frac{\partial F_{0e}}{\partial v_x} + \frac{\partial F_{0i}}{\partial v_x}\right]\Bigg|_{\omega_0/k} \,, \tag{46}$$

where $\omega_0/k = \alpha c_s$ and $\alpha = 1/\sqrt{1+k^2\lambda_D^2}$. For F_0 being Maxwellian, we have $\partial F_{0i}/\partial v_x = -(v_x/v_i^2)F_{0i}$ and $\partial F_{0e}/\partial v_x = -[(v_x - v_d)/v_e^2]F_{0e}$. Substituting into the above equation, we find

$$\begin{aligned}\frac{\mu}{\omega_0} =& \frac{\sqrt{\pi}\alpha^3 c_s^3}{2\sqrt{2}}\left[\frac{m_i}{m_e}\left(\frac{v_d}{\alpha c_s} - 1\right)\frac{1}{v_e^3}e^{-(\alpha c_s - v_d)^2/2v_e^2} - \frac{1}{v_i^3}e^{-\alpha^2 c_s^2/2v_i^2}\right] \,, \\ \approx& \alpha^3\sqrt{\frac{\pi}{8}}\left[\sqrt{\frac{m_e}{m_i}}\left(\frac{v_d}{\alpha c_s} - 1\right) - \left(\frac{T_e}{T_i}\right)^{3/2} e^{-\alpha^2 T_e/2T_i}\right] \,.\end{aligned} \tag{47}$$

For zero drift velocity $v_d = 0$, the ion-acoustic waves always damp. The damping is strongest when $T_i \sim T_e$, where the damping is mostly due to the resonant ions. For $T_i \ll T_e$, there are too few resonant ions and the damping is mostly due to the electrons, which is much slower.

The problem gets more interesting when the electron drift velocity is comparable to the sound speed. In this case, the electrons amplify rather than damp the waves. The situation is illustrated in Figure 1. If the ion damping is weak enough, μ can be brought to positive value, which leads to

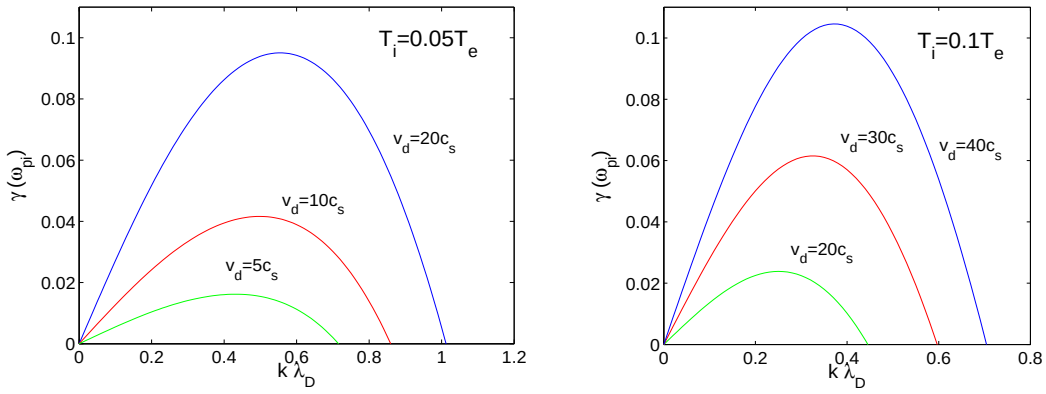

(a) $T_i = 0.05T_e$ (b) $T_i = 0.1T_e$

Figure 2: Growth rate of the ion-acoustic instability as a function of wave number $k\lambda_D$ for $T_i = 0.05T_e$ (a) and $T_i = 0.1T_e$ (b). Green, red and blue lines label different values of v_d, as marked in the figures. Growth rate is nomalized to the ion plasma frequency ω_{pi}.

Table 1: Scales and Parameters for the Ion-Acoustic Instability

Quantity	Definition	Meaning	Type
ω_{pi}	$\sqrt{m_e/m_i}\omega_{pe}$	ion plasma frequency	basic scale
c_s	$\sqrt{m_e/m_i}v_e$	sound speed	
λ_D	$v_e/\omega_{pe} = c_s/\omega_{pi}$	Debye length	
ω_{pe}	$\sqrt{4\pi n_0 e^2/m_e}$	electron plasma frequency	derived scale
v_i	$\sqrt{kT_i/m_i}$	ion thermal velocity	
v_e	$\sqrt{kT_e/m_e}$	electron thermal velocity	
T_i/T_e	-	ion temperature	parameter
v_d/c_s	-	drift velocity	

exponential growth of ion-acoustic waves. This is called the **ion-acoustic instability**. The critical drift speed v_{dc} above which the instability sets in sensitively depends on the ion temperature. For $T_i \approx T_e$, v_{dc} has to be comparable to v_e, while for $T_i \ll T_e$, one just needs $v_{dc} > c_s$. Figure 2 shows the growth rate of the ion-acoustic instability at two different ion temperatures. Note that the fastest growing wave length is comparable to the Debye length λ_D (hence it is a plasma micro-instability), and the corresponding growth rate is typically a few percent of the ion plasma frequency.

The ion-acoustic instability is the main mechanism we will consider as the source of anomalous resistivity. It is convenient for theoretical purposes to sort out various scales of the problem and the model parameters. We pick the ion plasma frequency ω_{pi}, the sound speed v_e and the Debye length λ_D as the characteristic time, velocity and length scales. In Table 1, we provide a list of other relevant scales and model parameters for the ion-acoustic instability problem, as well as for the rest of this report.

3 Wave-Particle Interaction

We have seen that plasma waves can damp or grow by resonant interactions between the waves and the particles. By energy conservation, particles gain or lose energy which modifies the particle distribution function. In this section, we study wave-particle interaction in more detail, where the change in particle distribution function is studied in parallel with wave damping and growth. More details can be found in the books by Galeev & Sagdeev (1969) and Diamond et al. (2010).

3.1 Quasi-linear Theory of Particle-Wave Interaction

The response of the particle distribution function to plasma waves is generally described as a diffusion process in the velocity space. To show this, we first consider the particle trajectories in a monochromatic wave. Assuming the amplitude of the electric field is a constant, we have $E = E_0 \sin(kx - \omega_0 t)$, corresponding to electrostatic potential $E_0 \cos(kx - \omega_0 t)/k$. In a frame co-moving with the wave, the particle energy is given by

$$\mathscr{E} = mv^2/2 - eE_0 \cos(kx)/k \ . \tag{48}$$

Particles with energy $\mathscr{E} < 0$ (or $\Delta v < \sqrt{eE/mk}$) will be trapped and oscillate in the wave similar to a harmonic oscillator, with orbital time scale to be

$$\tau_b = 1/k\Delta v = \sqrt{m/eE_0 k} \ . \tag{49}$$

In reality, waves can be thought of as a series of wave packets, whose autocorrelation time is

$$\tau_{ac} = 1/k|v_{ph} - v_g| \ . \tag{50}$$

where v_{ph} and v_g are the phase and group velocities of the wave. If the autocorrelation time τ_{ac} of the waves is shorter than the particle bouncing time τ_b, particles whose velocity is in the vicinity of v_{ph} will receive random kicks as the wave packets pass by, which leads to diffusion in the velocity space. Conditions for $\tau_{ac} \ll \tau_b$ is equivalent to $\Delta v \ll |v_{ph} - v_g|$, which requires the wave to be dispersive such that $v_g \neq v_{ph}$ and the wave amplitude to be not too large. We note that the ion-acoustic wave is not very dispersive for small k, which should be made caution.

Assuming the stochasticity condition $\tau_{ac} \ll \tau_b$ is valid, we describe the quasi-linear theory of wave-particle interaction below (Galeev & Sagdeev, 1969). We assume the system is in equilibrium state described by $F_0(v_x)$ for $t < 0$. At $t = 0$, the system is perturbed which generates plasma waves with a range of wave numbers. For each wave number, the electric field strength is given by $\overline{E}(k,t)$, whose amplitude varies as some known function of t.

We start by carrying out a spatial Foruier transformation as in equation (19), but keeping the non-linear terms

$$\frac{\partial \overline{F}(k)}{\partial t} + \mathrm{i}kv_x \overline{F}(k) + \frac{q}{m}\overline{E}(k)\frac{\partial F_0}{\partial v_x} = -\frac{q}{m}\int \overline{E}(k-k')\frac{\partial \overline{F}(k')}{\partial v_x}\left[1 - \frac{\delta(k')}{L}\right]dk' \ . \tag{51}$$

where L is the size of the system, and for $t > 0$, $F_0 = F_0(v_x, t) = \overline{F}(k = 0, v_x, t)/L$ is evolutionary.

For $k = 0$, note that $\overline{E}(k = 0) = 0$, we have

$$\frac{\partial \overline{F}(0)}{\partial t} = L\frac{\partial F_0}{\partial t} = -\frac{q}{m}\int \overline{E}(-k)\frac{\partial \overline{F}(k)}{\partial v_x}dk \ . \tag{52}$$

In the long term we are interested in the evolution of F_0, while $k \neq 0$ modes rapidly oscillate and average to zero. To obtain the evolution of $\overline{F}(k)$, we can neglect the non-linear terms in equation (51) since they are of higher order and obtain

$$\overline{F}(k, v_x, t) = -\frac{q}{m}\int_0^t \overline{E}(k,t')\frac{\partial F_0}{\partial v_x}e^{\mathrm{i}kv_x(t'-t)}dt' \ . \tag{53}$$

Substituting the above equation to equation (52), we obtain

$$\frac{\partial F_0}{\partial t} = \frac{q^2}{m^2 L}\frac{\partial}{\partial v_x}\int_k \overline{E}(-k,t)dk \int_0^t \overline{E}(k,t')\frac{\partial F_0}{\partial v_x}e^{\mathrm{i}kv_x(t'-t)}dt' \ . \tag{54}$$

In the next, we take the WKB approximation in which F_0 varies only slightly over one wave period and the wave damping/growth time scale. Therefore, we have

$$\overline{E}(k,t) = \overline{E}(k,0)\exp\left\{\int_0^t [-\mathrm{i}\omega(k)+\mu(k,t')]dt'\right\} , \tag{55}$$

where ω and μ are readily available from the linear perturbation theory. Substituting (55) into (54), we find

$$\frac{\partial F_0}{\partial t} = \frac{q^2}{m^2}\frac{\partial}{\partial v_x}\int_0^t dt' \int_k dk\overline{I}(k,t)\exp\left[-i[kv_x-\omega(k)](t-t') - \int_{t'}^t \mu(k,t'')dt''\right]\frac{\partial F_0(v_x,t')}{\partial v_x} \ , \tag{56}$$

where we have used $\overline{E}(-k) = \overline{E}(k)^*$, and $\overline{I}(k,t) \equiv |\overline{E}(k,t)|^2/L$. Now we assume that the wave spectrum is wide, i.e., $\Delta(kv_x-\omega(k)) \gg \mu(k,\tau_R^{-1})$ [where τ_R is the relaxation time for $F_0(v_x,t)$]. As a consequence, when $(t-t')$ is not small [compared with $\omega(k)$], the integral over k gives a vanishing result because of phase mixing. Therefore, most contribution to the k integral comes from $t' \to t$, for which reason we can safely replace $\mu(k,t'')$ by $\mu(k,t)$, and $F_0(k,v_x,t')$ by $F_0(k,v_x,t)$. Then, we carry out the integration over t' and obtain

$$\frac{\partial F_0}{\partial t} = \frac{q^2}{m^2}\frac{\partial}{\partial v_x}\int_k dk\overline{I}(k,t)\frac{1-\exp\left[-\mathrm{i}(kv_x-\omega)t-\mu t\right]}{\mathrm{i}(kv_x-\omega)+\mu}\frac{\partial F_0}{\partial v_x} \ . \tag{57}$$

As one integrates over k, we have the asymptotic relation

$$\frac{1-\exp\left[-\mathrm{i}(kv_x-\omega)t-\mu t\right]}{\mathrm{i}(kv_x-\omega)+\mu} = P\frac{1}{\mathrm{i}(kv_x-\omega)+\mu} + \pi\delta(kv_x-\omega) \ , \tag{58}$$

where P means principal value. With this relation, we can reduce equation (57) to the form

$$\frac{\partial F_0}{\partial t} = \frac{\partial}{\partial v_x}\left[D(v_x)\frac{\partial F_0}{\partial v_x}\right] , \tag{59}$$

where

$$D(v_x) = \frac{q^2}{m^2}\int_k dk\overline{I}(k,t)\left\{P\frac{\mu(k,t)}{[kv_x-\omega(k)]^2+\mu(k,t)^2} + \pi\delta[kv_x-\omega(k)]\right\} . \tag{60}$$

In equation (60), the term with a delta function is positive definite and corresponds to the smoothing of the distribution function due to resonant wave-particle interaction. This is an irreversible process. The term with the principal value describes a reversible process, representing the response of non-resonant particles to the waves. Physically, the wave energy is the sum of the energy from the electromagnetic field, and the particle kinetic energy associated with the waves. This term represents the latter part, and it grows or decay with the field energy. Below we elaborate these points by working out the energy and momentum exchanges between particles and waves.

The total energy of in the plasma can be decomposed in two ways. First, the energy is partitioned between resonant particles and waves. The rate of energy change due to resonant particles is given by

$$\begin{aligned}\frac{d\mathscr{E}_p}{dt} &= \int \frac{1}{2}mv_x^2\frac{\partial}{\partial v_x}\left[D_r(v_x)\frac{\partial F_0}{\partial v_x}\right]dv_x = -\int mv_x D_r(v_x)\frac{\partial F_0}{\partial v_x}dv_x \\ &= -\frac{\pi q^2}{m}\int dk\int v_x\overline{I}(k,t)\frac{\partial F_0}{\partial v_x}\delta[kv_x-\omega(k)]dv_x \\ &= -\frac{\pi q^2}{m}\int dk\frac{\omega(k)}{k^2}\overline{I}(k,t)\frac{\partial F_0}{\partial v_x}\bigg|_{\omega/k} ,\end{aligned} \tag{61}$$

where D_r represents the resonant part of the diffusion coefficient. For the waves, we have from equations (36) and (40)

$$\frac{d\mathscr{E}_w}{dt} = \int_k dk[2\mu(k)]\frac{\overline{I}(k)}{4\pi} = \frac{\pi q^2}{m}\int_k dk\frac{\omega(k)}{k^2}\overline{I}(k)\frac{\partial F_0}{\partial v_x}\bigg|_{\omega/k} . \tag{62}$$

Evidently, the total energy is conserved. Similarly, one can show that total momentum is conserved

$$\frac{d\mathscr{P}_p}{dt} = \int mv_x\frac{\partial}{\partial v_x}\left[D_r(v_x)\frac{\partial F_0}{\partial v_x}\right]dv_x = -\frac{\pi q^2}{m}\int\frac{dk}{k}\overline{I}(k,t)\frac{\partial F_0}{\partial v_x}\bigg|_{\omega/k} , \tag{63}$$

$$\frac{d\mathscr{P}_w}{dt} = \int_k dk\frac{2\mu(k)k}{\omega}\frac{\overline{I}(k)}{4\pi} = \frac{\pi q^2}{m}\int_k\frac{dk}{k}\overline{I}(k)\frac{\partial F_0}{\partial v_x}\bigg|_{\omega/k} . \tag{64}$$

Therefore, wave-particle interaction effectively exchange energy between particles and waves.

The other way is to divide the total energy into energy in the particles and energy in the field. The change in the field energy is simply half the rate of equation (62) since field energy is $E^2/8\pi$, which further implies the energy in the non-resonant particles associated with the waves is equal to the field energy, as expected. Note that electrostatic field does not carry momentum, therefore, the momentum is partitioned between resonant and non-resonant particles.

3.2 Non-linear Theory of Wave-Particle Interaction

The effect of non-linear wave damping becomes important when the wave amplitude becomes larger. The non-linear wave damping can be considered as the energy exchange process between two wave modes (k,ω), (k',ω') and a particle which is in resonance with the beat frequency of the two waves $v = (\omega-\omega')/(k-k')$. In this subsection we calculate the rate of non-linear wave damping and its effect on the particle distribution function.

A full derivation of the non-linear theory is a bit lengthy. Below we outline the main steps of the derivation from Manheimer & Dupree (1968). An alternative derivation is given by Galeev & Sagdeev (1969).

We work in the case of weak turbulence in infinite homogeneous plasma in 1D. In steady state, the electric fields can be expressed as

$$E(x,t) = \int dk\widetilde{E}(k)\exp\left[\mathrm{i}(kx-\omega t+\phi_k)\right] , \tag{65}$$

where $\omega=\omega(k)$ is determined from the dispersion relation, and is real in sustained turbulence, ϕ_k is the random phase. Note that since the electric field is real, we have $E(k)=E^*(-k)$, $\omega(k)=-\omega(-k)$, $\phi_k=-\phi_{-k}$.

To find the diffusion coefficients, we consider the particle trajectories due to stochastic forcing from the electric field

$$\frac{dv}{dt} = F(t) = \frac{q}{m}E[x(t),t] . \tag{66}$$

Once $F(t)$ is known, the diffusion coefficient is simply

$$D = \frac{1}{2}\int_{-\infty}^{\infty} < F(t+\tau)F(t) > d\tau , \tag{67}$$

where the bracket means ensemble average.

For weak turbulence, we can expand the particle trajectory in series as $x(t)=x_0(t)+x_1(t)+...$, where $x_0(t)=x_s+vt$, and the corresponding force expansion is $F(t)=F_1(t)+F_2(t)+....$ More explicitly, we have

$$\begin{aligned} F_1(t) &= \frac{dv_1}{dt} = \frac{q}{m}\int dk\widetilde{E}(k)\exp[\mathrm{i}(kx_s+\phi_k)]\exp[\mathrm{i}(kv-\omega)t] , \\ x_1(t) &= -\frac{q}{m}\int\frac{dk\widetilde{E}(k)}{(kv-\omega)^2}\exp[\mathrm{i}(kx_s+\phi_k)]\exp[\mathrm{i}(kv-\omega)t] . \end{aligned} \tag{68}$$

Using the definition (67), we find the second order diffusion coefficient

$$\begin{aligned} D_2(v) &= \frac{q^2}{2m^2}\int d\tau \int dk dk' \widetilde{E}(k)\widetilde{E}(k') e^{\mathrm{i}[(k+k')(x_s+vt)-(\omega+\omega')]} e^{\mathrm{i}(\phi_k+\phi_{k'})} e^{\mathrm{i}(k'v-\omega')\tau} \\ &= \frac{\pi q^2}{m^2}\int dk \widetilde{I}(k)\delta(kv-\omega) \ , \end{aligned} \tag{69}$$

where the random phase assumption with ensemble average enforces the selection rule $k' = -k$, and we have used the identity $\int d\tau e^{\mathrm{i}\omega\tau} = 2\pi\delta(\omega)$. Obviously, the above equation is identical to the resonant part of equation (60), as expected.

To the next order, we have

$$\begin{aligned} F_2(t) &= \frac{q}{m}\int dk E(k)[\mathrm{i}kx_1(t)]\exp[\mathrm{i}(kx_s+\phi_k)]\exp[\mathrm{i}(kv-\omega)t] \\ &= \frac{-\mathrm{i}q^2}{m^2}\int dk dk' \frac{kE(k)E(k')}{(k'v-\omega')^2}\exp[\mathrm{i}((k+k')x_s+(\phi_k+\phi_{k'}))]\exp[\mathrm{i}((k+k')v-(\omega+\omega'))t] \ . \end{aligned} \tag{70}$$

With the random phase assumption, the next order diffusion coefficient is D_4. After some algebra, we find

$$\begin{aligned} D_4 &= \frac{\pi q^4}{2m^4}\int dk dk' \widetilde{I}(k)\widetilde{I}(k')\left[\frac{k}{(k'v-\omega')^2}+\frac{k'}{(kv-\omega)^2}\right]^2 \delta[(k+k')v-(\omega+\omega')] \\ &= \frac{\pi q^4}{m^4}\int_{k>0} dk dk' \widetilde{I}(k)\widetilde{I}(k')\left[\frac{k+k'}{(k'v-\omega')(kv-\omega)}\right]^2 \delta[(k+k')v-(\omega+\omega')] \ , \end{aligned} \tag{71}$$

where in the second equality we have substituted $v = (\omega+\omega')/(k+k')$, which leads to $k'v-\omega' = \omega-kv$. Note that now we have taken $k > 0$. The integral with $k' > 0$ corresponds to the non-linear wave-particle interaction in which a wave (k,ω) is converted to (k',ω') via beat resonance with particles moving at velocity $(\omega+\omega')/(k+k')$, while the integral with $k' < 0$ corresponds to conversion to $(|k'|,|\omega'|)$ at resonance velocity $(\omega-|\omega'|)/(k-|k'|)$. We will treat these two cases separately, and for the latter situation, we set $k' \to -k'$, $\omega' \to -\omega'$, and the integral on k' goes from 0 to ∞.

Next, we discuss the back reaction of the particles to the waves. Consider the interaction between two waves with wave numbers k and k'. By energy and momentum conservation, we have

$$(\omega \pm \omega')\dot{N}_k(k') = -\int \frac{1}{2}mv_x^2 \frac{\partial}{\partial v_x}\left[D_4(k,k')\frac{\partial F_0}{\partial v_x}\right]dv_x \ , \tag{72}$$

$$(k \pm k')\dot{N}_k(k') = -\int mv_x \frac{\partial}{\partial v_x}\left[D_4(k,k')\frac{\partial F_0}{\partial v_x}\right]dv_x \ , \tag{73}$$

where $D_4(k,k')$ is the integrant of equation (71), N_k is defined in equation (35), and the plus/minus sign correspond to the case for $k' > 0$ and $k' < 0$ respectively. In the above equations, we have implicitly used the **Manley-Rowe relations**, and here it guarantees that $\dot{N}_k(k') = \pm\dot{N}_{k'}(k)$. From the above equations, we obtain

$$\begin{aligned} \dot{N}_k(k') =& \frac{\pi q^4}{m^3}\widetilde{I}(k)\widetilde{I}(k')\left[\frac{1}{(kv_x-\omega)^4}\frac{\partial F_0}{\partial v_x}\bigg|_{v_x=\frac{\omega+\omega'}{k+k'}} + \frac{\mathrm{sgn}(k-k')}{(kv_x-\omega)^4}\frac{\partial F_0}{\partial v_x}\bigg|_{v_x=\frac{\omega-\omega'}{k-k'}}\right] \\ =& \frac{\widetilde{I}(k)\widetilde{I}(k')}{16\pi n_0 m v_T^2}\left[\frac{\omega_p^4 v_T^2}{(kv_x-\omega)^4}\frac{1}{n_0}\frac{\partial F_0}{\partial v_x}\bigg|_{v_x=\frac{\omega+\omega'}{k+k'}} + \frac{\omega_p^4 v_T^2}{(kv_x-\omega)^4}\frac{\mathrm{sgn}(k-k')}{n_0}\frac{\partial F_0}{\partial v_x}\bigg|_{v_x=\frac{\omega-\omega'}{k-k'}}\right] \ . \end{aligned} \tag{74}$$

For conciseness, we define the quantity in the bracket as $A(k,k')$. Integrating over all possible combinations, and apply to the ion-acoustic turbulence, we find the non-linear damping rate for waves with wave number k as

$$\begin{aligned} \frac{1}{\omega_{pi}}\frac{d\widetilde{I}(k)}{dt} &= \frac{4\pi\omega^3}{\omega_{pi}^3}\int_0^\infty dk'[\dot{N}_{ek}(k')+\dot{N}_{ik}(k')] \\ &= \frac{\omega^3}{4\omega_{pi}^3}\widetilde{I}(k)\int_0^\infty dk'\widetilde{I}(k')\left[\frac{A_e(k,k')}{n_0 m_e v_e^2}+\frac{A_i(k,k')}{n_0 m_i v_i^2}\right] \ , \end{aligned} \tag{75}$$

where we have used equations (36) and (45).

3.3 Wave Energy Spectrum

The key to calculate the anomalous resistivity in our model is to obtain a (quasi) steady state energy spectrum of ion-acoustic waves. Ion-acoustic waves are excited by the ion-acoustic instability (§2.4) and damped by linear and non-linear Landau damping as discussed in §2.3 and §3.2. To determine the wave energy spectrum, one has to take into account another non-linear effect: wave-wave interaction. To the lowest order, the three interacting wave must satisfy $\boldsymbol{k}' + \boldsymbol{k}'' = \boldsymbol{k}$ and $\omega' + \omega'' = \omega$. This can not be satisfied by three ion-acoustic modes since its dispersion relation (32) is not linear for $k \leq \lambda_D$. Since we are discussing the plasma waves with zero guide field, the only possibility for wave-wave interaction is by interacting the ion-acoustic wave with two plasma oscillation modes. However, there is no effective way to excite plasma oscillation, therefore, we expect wave-wave interaction to be unimportant and neglect this effect. Below we calculate the wave energy spectrum based on linear and non-linear Landau damping.

The linear growth rate of the ion-acoustic instability is given in equation (47). Combined with the non-linear damping rate, we obtain

$$\frac{1}{\omega_{pi}}\frac{d\widetilde{I}(k)}{dt} = 2\frac{\mu(k)}{\omega_{pi}}\widetilde{I}(k) + \frac{\omega^3}{4\omega_{pi}^3}\widetilde{I}(k)\int_0^\infty dk'\widetilde{I}(k')\left[\frac{A_e(k,k')}{n_0 m_e v_e^2} + \frac{A_i(k,k')}{n_0 m_i v_i^2}\right] . \tag{76}$$

In steady state, $d\widetilde{I}(k)/dt = 0$ for all ks. Therefore, we find

$$-\int_0^\infty dk'\widetilde{I}(k')\left[\frac{A_e(k,k')}{n_0 m_e v_e^2} + \frac{A_i(k,k')}{n_0 m_i v_i^2}\right] = \frac{8\mu(k)\omega_{pi}^2}{\omega^3} . \tag{77}$$

The solution of this integration equation gives the wave amplitude.

In reality, one expects the electrons play an insignificant role in the non-linear wave damping because its distribution function is flat. Moreover, the wave-particle interaction in (72) with the plus sign does not conserve total number of waves, and we drop the corresponding terms in our calculation. The remaining terms, however, becomes very stiff as k is small due to the $1/(kv_x - \omega)^4$ dependence, which is due to the fact that the ion-acoustic wave is not very dispersive for small k. This makes it numerically challenging to solve the integral equation (77). As we have discussed before, the particle-wave interaction can no longer be considered as a diffusion process under such circumstances. In practice, this is handled by analytically integrating k' across the stiff region in the vicinity of k, where thanks to the $\mathrm{sgn}(k - k')$ factor, the stiff terms largely average out, while the net effect is still wave damping.

In Figure 3, we show the *preliminary* calculation of the wave spectrum from the integral equation (77) for two different ion temperatures. The wave spectrum peaks near the cutoff wave length of the ion-acoustic instability, which is close to the Debye length, and falls off sharply for slightly larger k due to the efficient energy transfer from large to small wave numbers. For smaller k, the ion-acoustic wave becomes less dispersive, and the damping due to the $1/(kv_x - \omega)^4$ factor becomes stronger and stronger. Moreover, as we have discussed at the beginning of this section, at smaller k, the evolution of the particle distribution function may not be described by a diffusion process. The suppression of the wave spectrum at small k makes this violation less concerning. The energy in the weak turbulence is an increasing function of v_d, because the growth rate increases with v_d (see Figure 2), while the wave damping rate is independent of v_d.

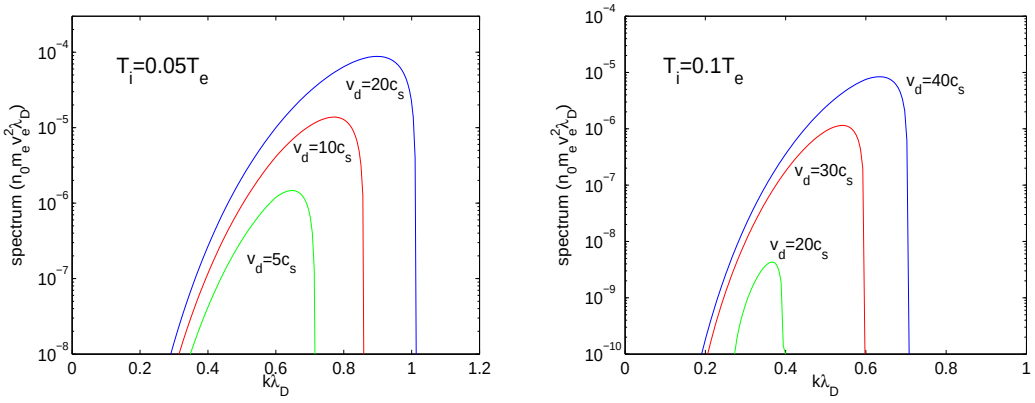

(a) $T_i = 0.05T_e$ (b) $T_i = 0.1T_e$

Figure 3: The calculated wave energy spectrum in natural unit $n_9 m_e v_e^2 \lambda_D$ for $T_i = 0.05T_e$ (a) and $T_i = 0.1T_e$ (b). Green, red and blue lines label different values of v_d, as marked in the figures.

4 Anomalous Resistivity for Sweet-Parker Reconnection

4.1 Momentum Transport and Anomalous Resistivity

Given the wave amplitudes over the spectrum, we are able to calculate the rate of momentum transport and obtain the anomalous resistivity. In the ion-acoustic turbulence, electrons lose momentum while the ions gain momentum, both effects tend to reduce the drift velocity. Equivalently, an electric field along the current is needed to maintain the drift velocity in the steady state. The conductivity/resistivity is then obtained simply from the Ohm's law. More specifically, we have

$$\frac{d\mathscr{P}_e}{dt} = -n_0 e E_e^{\rm eff} \ , \qquad \frac{d\mathscr{P}_i}{dt} = n_0 e E_i^{\rm eff} \ , \tag{78}$$

where $\mathscr{P}$ is the momentum density for electrons and the ions, $E^{\rm eff}$ is the effective electric field. Note that the effective electric field for electrons and the ions does not necessarily be the same. However, since electrons are much more mobile than the ions, the anomalous resistivity mainly arises from the electrons, therefore, we take $E^{\rm eff} = E_e^{\rm eff}$. By definition, the anomalous resistivity is

$$\eta^{\rm eff}(j) = \frac{c^2}{4\pi\sigma^{\rm eff}} = \frac{E^{\rm eff}(j)c^2}{4\pi j} = \frac{c^2}{4\pi n_0^2 e^2}\frac{1}{v_d}\left|\frac{d\mathscr{P}_e}{dt}\right| . \tag{79}$$

Here we emphasize the strong dependence of $\eta^{\rm eff}$ and $E^{\rm eff}$ on the current density j.

The momentum loss rate on the electrons is dominated by the linear Landau damping given by equations (63)

$$\frac{1}{\omega_{pe}}\frac{d\mathscr{P}_e}{dt} = -\frac{n_0 m_e v_e}{4}\int \frac{dk\overline{I}(k,t)}{n_0 m_e v_e^2}\frac{1}{k\lambda_D}\frac{v_e^2}{n_0}\frac{\partial F_{0e}}{\partial v_x}\bigg|_{\omega/k} , \tag{80}$$

The anomalous resistivity is then

$$\eta^{\rm eff}(j) = \frac{c^2}{\omega_{pi}}\frac{c_s}{4v_d}\int \frac{dk\overline{I}(k,t)}{n_0 m_e v_e^2}\frac{1}{k\lambda_D}\frac{v_e^2}{n_0}\frac{\partial F_{0e}}{\partial v_x}\bigg|_{\omega/k} . \tag{81}$$

In Figure 4, we show the calculated anomalous resistivity as a function of v_d from the wave spectrum obtained in the previous subsection. We see that $\eta^{\rm eff}$ sensitively depends on v_d at the onset of the ion-acoustic instability, and the curve flattens as v_d approaches $v_e \approx 40c_s$. This relation is in accordance with the dependence of the growth rate μ on v_d.

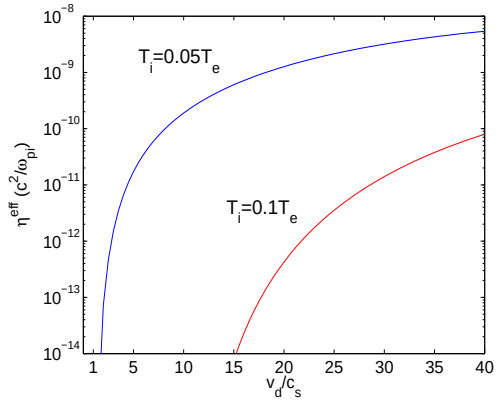

Figure 4: The preliminary calculation of the anomalous resistivity $\eta^{\rm eff}$ as a function of the electron drift speed v_d for two different ion temperatures, as labeled in the figure. $\eta^{\rm eff}$ is normalized to c^2/ω_{pi}.

4.2 Sweet-Parker Reconnection with Anomalous Resistivity

We have introduced the Sweet-Parker reconnection model in §1.1 where the resistivity is constant. As we show before, anomalous resistivity strongly depends on the drift speed, or the current density. One step forward is to improve the Sweet-Parker model by including the current dependence on the resistivity. More specifically, equation (4) is replaced by a transcendental equation

$$\delta \approx \sqrt{\frac{\eta^{\rm eff}(j)L}{v_A}}, \tag{82}$$

where $j = n_0 e v_d = cB_0/4\pi\delta$ further depends on δ.

Our anomalous resistivity calculation has resulted a relation of $\eta^{\rm eff}$ as a function of v_d. We just need another relation between $\eta^{\rm eff}$ and v_d based on the Sweet-Parker model, which can be found by rewritten equation (4) as $\eta^{\rm eff} = (v_A/L)\delta^2$. Renormalizing this equation, we find

$$\frac{\eta^{\rm eff}}{c^2/\omega_{pi}} = \frac{v_A^3}{c_s^2\omega_{pi}L}\left(\frac{c_s}{v_d}\right)^2 . \tag{83}$$

Therefore, in natural unit, $\eta^{\rm eff} \propto 1/v_d^2$ from the Sweet-Parker model. The coefficient $v_A^3/c_s^2\omega_{pi}L$ could be estimated from the physical environment.

In Figure 5, we overplot the additional relation from the Sweet-Parker model, with the coefficient estimated from the environment in solar flares and the earth magnetosphere (see §1.2). The intersection between the solid and dashed line then gives the solution of the transcendental equation.

At this point, we are ready to compare our model of anomalous resistivity with observations. As an illustration, we take $T_i = 0.05T_e$ in the calculation. In the case of solar flare, we find

$$\eta_O \sim 10{\rm cm}^2{\rm s}\ , \qquad \eta^{\rm eff} \sim 7\times 10^3{\rm cm}^2{\rm s}\ . \tag{84}$$

Note that the anomalous resistivity is substantially larger than the microscopic Ohmic resistivity. However, it only shortens the reconnection time scale by a factor of about 30, and the resulting reconnection rate is still far from the observational constraints.

Similarly, for the Earth's magnetosphere, we have

$$\eta_O \sim 2\times 10^4{\rm cm}^2{\rm s}\ , \qquad \eta^{\rm eff} \sim 10^6{\rm cm}^2{\rm s}\ . \tag{85}$$

Again, we have found a somewhat larger resistivity, but it is still too small to match the observations.

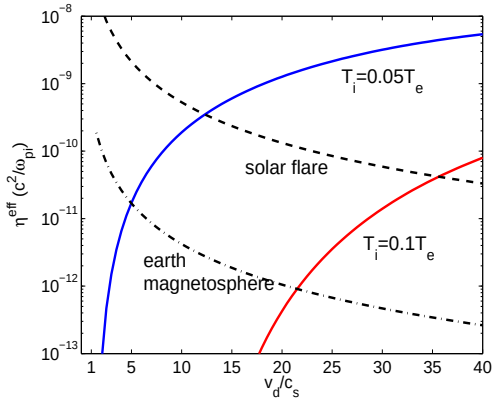

Figure 5: Same as Figure 4, but with additional relation from the Sweet-Parker model (83) shown in black dashed curves, where the coefficient is estimated from the environment in solar flares and the Earth magnetosphere.

5 Summary

In this report, we have constructed a 1D toy model for non-relativistic collisionless reconnection of ion-electron plasma. It is a toy model in several aspects. First of all, being a 1D model, we have ignored the layer structure of the reconnecting current sheet. In particular, the current density across the current layer is non-uniform, and magnetic field is non-zero and switches sign across the layer. Our perturbation analysis ignores the magnetic field and current gradients, and only considers perturbations along the direction of current, which is far from being realistic. Moreover, 1D model excludes the tearing mode instability, which distorts and corrugates the current sheet.

Secondly, we have ignored the guide field. The guide field is the background field which is superimposed to the oppositely directed reconnecting field lines. Adding a guide field makes the reconnection problem more tractable if the guide field strength is comparable to or stronger than B_0, with the drift-kinetic equations involved. This is a possible extension for future work.

Finally, our calculation of the ion-acoustic turbulence spectrum needs to be improved. In particular, the calculation of non-linear wave-particle interaction is only approximate, where for $k \ll 1/\lambda_D$, the wave dispersion relation is linear and quasi-linear theory tends to fail. Moreover, we have assumed that both electrons and the ions are thermal, and we have ignored the change of particle distribution function due to the wave-particle interactions. These are both unjustified, and the presence of non-thermal particles from the solar flares clearly makes our assumption questionable.

Despite all these simplifications and approximations, we have pedagogically presented the basic physics and the main steps for the calculation of anomalous resistivity. Resistivity arises from momentum exchange. In the case of microscopic Ohmic resistivity, momentum exchange is mediated by electron collisions. In the collisionless regime, momentum exchange can be mediated by wave-particle interaction. For Sweet-Parker reconnection, ion-acoustic waves are excited when the electron drift velocity in the current sheet exceeds a few times the sound speed. The wave excitation extracts energy and momentum from the electrons, which in turn produces anomalous resistivity. The wave damping is mostly due to non-linear wave-particle interaction, and wave momentum is dumped to the ions. The momentum exchange rate, hence $\eta^{\rm eff}$, is directly related to the wave spectrum.

Our preliminary calculation of the anomalous resistivity shows that it sensitively depends on the electron drift speed v_d when it just exceeds the threshold for the ion-acoustic instability. The dependence weakens as v_d approaches the electron thermal velocity. Matching the results with the

Sweet-Parker model, the resulting anomalous resistivity is generally several orders of magnitude larger than the Ohmic value. However, the calculated anomalous resistivity is still much smaller than required to fit the observations. This is not too surprising given the approximate nature of our toy model. Future work with more careful and detailed analysis may lead to better agreement.

I thank the organizers of the 2010 ISIMA held in University of California, Santa Cruz for hospitality and for providing this excellent opportunity of colaborative research. Special thanks to my faculty advisor Pat Diamond for mentoring my project and for patiently guiding me through the basics of plasma physics and magnetic reconnection.

References

Braginskii, S. I. 1965, Reviews of Plasma Physics, 1, 205

Diamond, P. H., Itoh, S-I., Itoh, K., 2010, Modern Plasma Physics, Vol.1, London, Cambridge University Press

Galeev, A. A., & Sagdeev, R. Z. 1969, Nonlinear Plasma Theory, New York: Benjamin

Hughes, W., 1995, Introduction to Space Physics, edited by M. Kivelson and C. Russell, London, Cambridge University Press

Kulsrud, R. M. 2005, Plasma physics for astrophysics, Princeton, NJ: Princeton University Press

Malyshkin, L. M., Linde, T., & Kulsrud, R. M. 2005, Physics of Plasmas, 12, 102902

Manheimer, W. M., & Dupree, T. H. 1968, Physics of Fluids, 11, 270

Parker, E. N. 1957, Journal of Geophysical Research, 62, 509

Petschek, H. E. 1964, NASA Special Publication, 50, 425

Sweet, P. A. 1958, Electromagnetic Phenomena in Cosmical Physics, 6, 123

Uzdensky, D., & Kulsrud, R. M. 2000, Physics of Plasmas, 7, 4018

Yamada, M., Kulsrud, R., & Ji, H. 2010, Reviews of Modern Physics, 82, 603

Zweibel, E. G., & Yamada, M. 2009, ARA&A, 47, 291